Self-Consistent Model of a High-Power Hall Thruster Plume

Alejandro Lopez Ortega, Ira Katz, Ioannis G. Mikellides, and Dan M. Goebel

***Abstract*— A new model of the plasma plume from Hall effect thrusters (HETs) has been developed for the purpose of more accurately predicting the interactions between future high-power thrusters and large high-voltage solar arrays, such as those being developed under NASA's Game Changing Technology awards by ATK and Deployable Space Systems. The HET plume mainly consists of two types of ions. The first are the energetic main beam ions produced upstream of the thruster acceleration zone. These are the dominant ion species along the thrust axis. The other group of ions have lower kinetic energy and are generated downstream of the acceleration zone from neutral xenon gas atoms by charge exchange (CEX) with main beam ions and by electron impact ionization. The neutral gas is due to neutral propellant atoms leaving the thruster and the hollow cathode without being ionized, and, in the case of laboratory testing, background neutrals present in the vacuum chamber. The new model uses the 2-D axisymmetric Hall thruster code, Hall2De, to self-consistently calculate the three major components of the plume in the vicinity of the thruster, which are the neutral gas atoms, high-energy beam ions, and low-energy ions. From the boundary computational region in the near plume, the Hall2De results are propagated to distances of tens of meters using a continuum hydrodynamic algorithm. This approach offers important advantages with respect to prior models of Hall thruster plumes, such as the NASA Electric Propulsion Interactions Code (EPIC), which uses an analytical fit to laboratory data from a single thruster for the main beam velocity boundary conditions at the channel exit. EPIC assumes that the neutral gas density emanates uniformly and isotropically from the channel exit. Low-energy ions are generated only by CEX; low-energy ions generated by electron impact are not included. The results for the far-field plume of a conceptual high-power thruster (H6) show important differences between EPIC and simulations using the new plume model. High-energy ions undergo less expansion in the azimuthal direction than in EPIC. This can be attributed to magnetic focusing of the beam. We also observe that the peak in low-energy ion density at approximately 90° from the thrust axis predicted by EPIC is moved downstream to angles from 70° to 80° when the new plume model is employed.**

***Index Terms*— Charge exchange (CEX), Hall thruster far plume, high-voltage solar arrays.**

I. Introduction

HALL effect thrusters (HETs) [1] are electric propulsion devices capable of producing specific impulse values in excess of 1500s by accelerating ions of a heavy species (such as xenon) through an electric field. In contrast to ion thrusters, ionization is produced by collisions of neutral atoms with electrons trapped in an magnetic field perpendicular to the electric field. HETs were originally developed in the Soviet Union and mainly marketed as low-power propulsion solutions for satellite station keeping. However, their high efficiency makes them suitable candidates for deep-space missions in which large impulses are required. These missions can only be enabled by the use of large solar panels that meet the power requirements of large electric propulsion devices (typically in the range of 6–20 kW). Major concerns in the operation of such devices are related to the interaction of charged particles with spacecraft surfaces. Ion sputtering can erode not only the walls of the thruster, changing its performance characteristics and shortening its life, but also other spacecraft surfaces. Charged particles can also cause interferences with communication's equipment. In deep-space missions, the large voltage applied to high-power solar arrays (especially when operated in direct drive) may result in performance losses due to parasitic current collection [2].

Assessment of erosion due to plume interactions with spacecraft usually begins by constructing a map of the ion density and current at distances of meters away from the thruster location. There exist a variety of numerical tools for examining the behavior of plasmas inside the acceleration channel of a Hall thruster and the near-plume region. The HPHall code [3] has been the reference algorithm for many years in the electric propulsion community. Hall2De [4] is a numerical algorithm developed at the Jet Propulsion Laboratory (JPL) that differs from HPHall in that it solves electron motion using full 2-D equations and uses a hydrodynamic approach for ion motion. The computational domains in these codes typically comprise distances of a few centimeters from the Hall thruster channel, and extending them to the geometry required for constructing a far-plume map would greatly increase the computational cost to the point that it will not be affordable to run these codes on workstation-class computers.

Multiple alternatives have been proposed to obtain plume models within affordable computational costs. Oh and Hastings [5] and Oh *et al.* [6] made use of particle-in-cell (PIC) [7] and direct simulation Monte Carlo (DSMC) [8] algorithms for computing a plume model far from the channel exit. The conditions at the channel exit were replicated by generating PIC macroparticles at a rate determined by the experimental measurements in the stationary plasma thruster-100 (SPT-100) [9]. This paper shows that the set of equations to be solved can be greatly simplified under

Manuscript received October 14, 2014; revised January 28, 2015; accepted May 15, 2015. Date of publication July 27, 2015; date of current version September 9, 2015. This work was supported by the Jet Propulsion Laboratory.

The authors are with the Jet Propulsion Laboratory, California Institute of Technology, Pasadena, CA 91109 USA (e-mail: alejandro.lopez.ortega@jpl.nasa.gov; ira.katz@jpl.nasa.gov; ioannis.g.mikellides@jpl.nasa.gov; dan.m.goebel@jpl.nasa.gov).

Color versions of one or more of the figures in this paper are available online at http://ieeexplore.ieee.org.

Digital Object Identifier 10.1109/TPS.2015.2446411

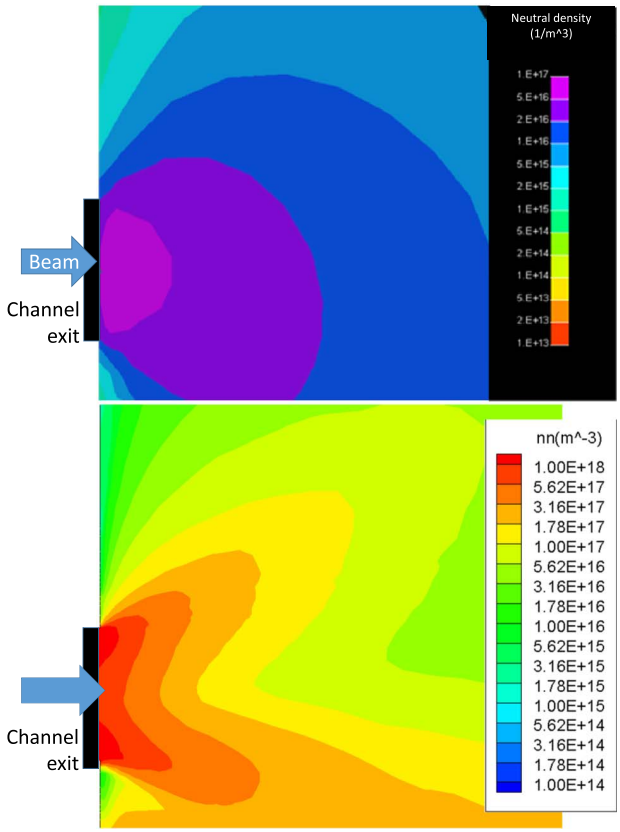

Fig. 1. Neutral density distribution as assumed in EPIC (top) and Hall2De (bottom). Large deviations from an isotropic distribution of neutral density occur in the near plume.

the verified assumptions that the Debye length and the effects of the presence of a magnetic field are small in the far-plume region. A similar approach was developed in [10] and used for comparison with data derived from in-space measurements of the SPT-100 thrusters onboard the Russian Express satellites. The NASA Electric Propulsion Interactions Code (EPIC) [11], [12] separates the ion population into two distinct species. The main beam ions, which have been accelerated through the electric field and have large kinetic energies, and the charge exchange (CEX) ions produced downstream of the acceleration region. In a CEX collision, a fast ion from the main beam interacts with a neutral in a way such that the ion becomes a neutral atom with high kinetic energy and the slow-moving neutral is ionized. This phenomenon effectively results in a change in magnitude and direction of the average linear momentum of the heavy particles and allows for slow ions to move in random directions, potentially backward, and pose a threat to spacecraft surfaces. In EPIC, main beam ions are modeled as a continuum fluid, while ions generated in CEX collisions make use of a PIC algorithm. This code employs the density and momentum profile at the channel exit of the SPT-140 Hall thruster for prescribing inflow boundary conditions and assumes an isotropic distribution of neutrals in the plume [Fig. 1(top)]. Electron-impact ionization is not accounted for in EPIC, and therefore the net number of neutral particles remains constant. Numerical simulations of the near plume using Hall2De [Fig. 1(bottom)] reveal that the neutral density in this region is far from isotropic since ionization is not negligible in the main beam close to the channel exit, where electron temperatures and plasma density are relatively large. Due to the wide variety of channel geometry and magnetic fields employed in modern Hall thrusters, these approximations may fall short, especially with magnetic fields in newer thrusters that strongly focus the ion beam to maximize thrust.

Analytical and experimental techniques for determining the far-plume map face multiple challenges. Analytical models [13], [14] are only available when large simplifications, such as considering a model in which all the particles emanate from a point in space, are considered. The experimental results [15]–[19] are constrained by the residual background pressure present in test chambers. The increased number of neutral atoms can effectively change the rate at which CEX collisions occur, substantially increasing ion sputtering of spacecraft surfaces. Hence, experimental measurements may be used for the validation of numerical plume models, but behavior in space is difficult to predict by the exclusive use of experimental means.

The algorithm proposed here offers multiple advantages with respect to previous efforts. The ion density and momentum are consistently obtained from simulations run with the Hall2De code. Thus, no hypothesis on the radial profile for density and fluxes at the channel exit is required. In addition, Hall2De has the built-in capability of simulating multiple fluids at once, so low-energy ions generated by CEX or ionization inside the computational domain of the Hall thruster solver are captured. In order to obtain an accurate distribution of the neutral density in the plume (Fig. 1), production of ions both through electron-neutral collisions and CEX is considered and the motion of neutral atoms is constructed consistently with the boundary conditions in the anode and thruster walls imposed in Hall2De.

This paper is structured as follows. Section II describes the numerical method that has been implemented in our plume model, devoting subsections to the computational domain, equations of motion, boundary, and initial conditions. In Section III, we show comparisons with EPIC simulations for a conceptual high-power Hall thruster (H6).

II. Numerical Method

A. Computational Domain

Our aim is to capture the density and energy of heavy ion particles over distances of several meters from the Hall thruster location. Since Hall thruster simulations using Hall2De typically extend to approximately 20 cm from the channel exit, it is necessary to formulate a new algorithm for far-plume simulations with an extended computational domain and a coarser grid topology in order to cover the region of interest.

The basic shape of the computational domain is outlined in Fig. 2. The inner cavity corresponds to the computational domain of the underlying Hall2De simulation (which comprises the thruster and the near plume up to 20 cm from the acceleration channel exit) in a way such that the boundaries of

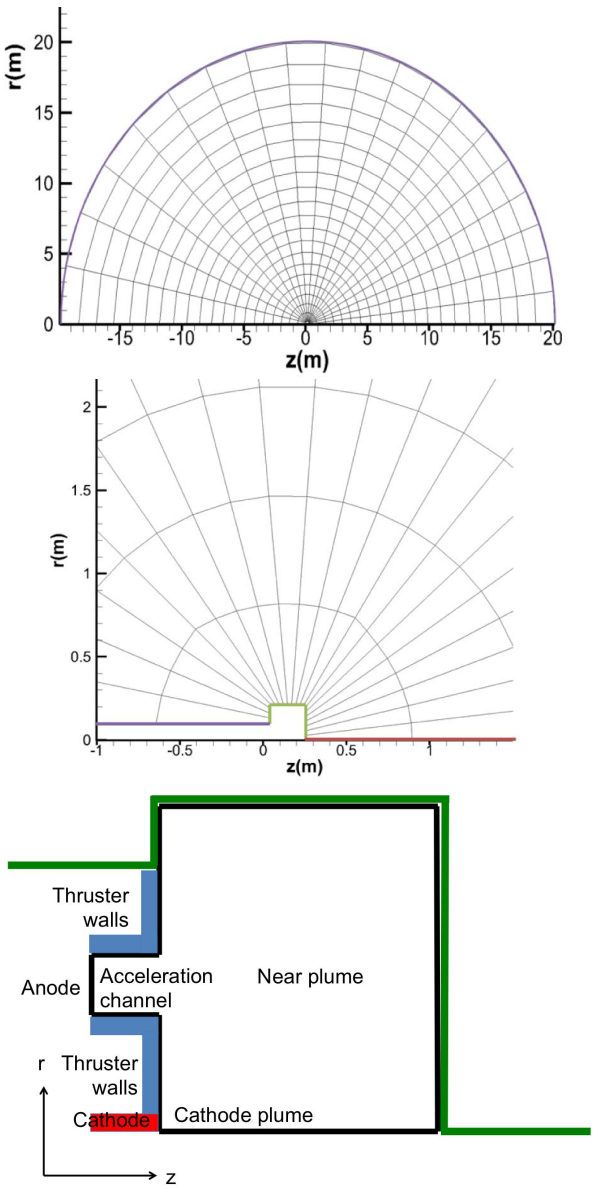

Fig. 2. Top: typical computational domain (low-resolution grid). Middle: detail of inflow boundary with different boundaries for the plume model, which are depicted as follows—red for centerline, magenta for outflow, and green for inflow conditions given by Hall2De simulations. Bottom: schematic of thruster geometry with centered-mounted cathode. Hall2De domain boundaries (black) and plume model domain boundaries (green). The Hall2De computational domain, which includes the near-plume region, fits in the central cavity of the plume model.

the plume model correspond to the outer boundaries (outflow) of the Hall2De domain. The boundary of the plume model that surrounds the cavity will be called inflow boundary condition hereinafter. The thruster beam moves to the right in the z-direction in this frame of reference. The radial direction r is measured with respect to the thruster axis of symmetry. There exists a centerline boundary at $r = 0$, so only one half of the whole region of interest needs to be numerically simulated. All the remainder boundaries are modeled as outflows. In Section II-C, a detailed definition of the coupling between outflow conditions for Hall2De and the inflow boundary conditions of the plume model is given. Corrections for cylindrical coordinates are implemented in the equations of motion in a way such that the computational domain roughly represents a sphere around the thruster location.

A series of rays and circles is employed to discretize the computational domain. The procedure described here is fully automatized in the code and requires only a few user inputs, such as the number of rays and circles. Other methods for passing the grid geometry to the plume model can be readily implemented, such as generating the grid in an external piece of software and having the plume model read a series of files containing a description of the grid topology. We start by dividing the inflow boundary in segments of approximately equal length, defining vertices between segments and at the corners. Each ray emanates from a vertex and follows the equation:

$$(z - z_i) = \tan(\alpha_i)(r - r_i) \tag{1}$$

where (z_i, r_i) are the vertex coordinates. The angle of the ray with respect to the z-axis (α_i) is progressively increased from 0 to π as the computational domain is swept in the counterclockwise direction. The increment in angle from ray to ray does not have to be linear. This feature is used to improve the aspect ratio of the computational cells as angle increments from ray to ray become larger as we move in the counterclockwise direction.

The circles are defined so that they linearly transition from a square shape that mimics the inflow boundary to a pure circular shape at a radius from the origin specified by the user (typically 1 m). This transition can be observed in Fig. 2 (also in Fig. 4), and it is included to avoid irregularly shaped cells close to the inflow boundary. The spacing of circles is controlled by a user input such that smaller cells with a better aspect ratio are generated close to the inflow boundary and coarser cells are generated as we move outward from the thruster location. It is worth noting that since the rays do not emanate from the same point in this automatized grid generation process, the resulting grid is not orthogonal in general. However, deviations from orthogonality decrease in cells far from the origin. A Newton–Raphson algorithm is employed to compute the intersections of rays and circles, and hence define the vertices, edges, and cells of the computational domain.

B. Equations of Motion

The far-plume algorithm takes advantage of the methods already implemented in the 2-D Hall thruster code Hall2De. Since Hall2De simulations are used to provide boundary conditions to the plume model, a brief description of this algorithm is in order. Equations of motion are solved independently for ions, electrons, and neutrals. Ions are treated using a hydrodynamic approach, which potentially leads to inaccuracies of the ion distribution in the plume as in reality, high-velocity beam ions do not equilibrate with low-velocity ions generated downstream of the acceleration region. To circumvent this difficulty, multiple ion populations that group ions of similar energy, called hereinafter fluids, can be defined in the algorithm. Brackets of energy are subsequently defined to separate the populations in a way such that gain of ions for a given population through ionization occurs only in regions where the plasma potential is comprised within the

bracket of that particular population. A typical example of this approach is to define two fluids in the simulation with a threshold of 50 V between the two for a thruster operating at a discharge voltage of 300 V. Under these conditions, the ions generated in the acceleration channel belong to fluid 1, while the ions generated in regions where the plasma potential is below 50 V are included in fluid 2. These two populations will follow their own equations of motion and interact only with one another through CEX collisions (i.e., in the previous example, if a fast ion undergoes a CEX collision with a neutral in a region where the plasma potential is below 50 V, the population of fast ions loses one ion that is transferred to the population of slow ions). If an infinite number of fluid populations could be considered, this algorithm would replicate the PIC results. Finally, each fluid can contain singly, doubly, and triply charged ions. For each species, density and momentum are computed using the isothermal hydrodynamic equations in the presence of an electric field

$$\frac{\partial n_{iC,iF}}{\partial t} + \nabla \cdot (n_{iC,iF}\mathbf{u}_{iC,iF}) = \dot{n}_{iC,iF} \tag{2}$$

$$\begin{aligned}\dot{n}_{iC,iF} = {} & b_{iF}(\phi)\left(\dot{n}_{iz,0\to iC,iF} + \sum_{jF=1,nF}\dot{n}_{\mathrm{CEX},iC,jF}\right) \\ & - \dot{n}_{\mathrm{CEX},iC,iF} + \sum_{jC<iC}\dot{n}_{iz,jC\to iC,iF} \\ & - \sum_{jC>iC}\dot{n}_{iz,iC\to jC,iF}\end{aligned} \tag{3}$$

$$\begin{aligned}&\frac{\partial}{\partial t}(n\mathbf{u})_{iC,iF} + \nabla\cdot(n\mathbf{uu})_{iC,iF} \\ &\quad = \frac{q_{iC}n_{iC,iF}\mathbf{E}}{m} - \frac{kT_i}{m_i}\nabla(n_{iC,iF}) + \mathbf{R}_{\mathrm{elastic},iC,iF} \\ &\quad + \mathbf{R}_{\mathrm{inelastic},iC,iF}\end{aligned} \tag{4}$$

$$\begin{aligned}\mathbf{R}_{\mathrm{inelastic},iC,iF} = {} & b_{IF}(\phi)\left(\dot{n}_{iz,0\to iC,iF} + \sum_{jF=1,nF}\dot{n}_{\mathrm{CEX},iC,jF}\right)\mathbf{u}_n \\ & - \dot{n}_{\mathrm{CEX},iC,iF}\mathbf{u}_{iC,iF} + \sum_{jC<iC}\dot{n}_{iz,jC\to iC,iF}\mathbf{u}_{jC,iF} \\ & - \sum_{jC>iC}\dot{n}_{iz,iC\to jC,iF}\mathbf{u}_{iC,iF}\end{aligned} \tag{5}$$

where *iC* and *iF* denote the charge state (i.e., singly, doubly, and triply charged ions, 1, 2, and 3, respectively) and the fluid number (up to 4), respectively. n is the number density, $\mathbf{u}$ is the velocity field, m is the ion atomic mass, k is Boltzmann's constant, q_{iC} is the charge of an ion particle in coulombs, and T_i is the ion temperature, considered isothermal and equal to the temperature of the thruster walls. The ion production term $\dot{n}$ and the inelastic drag $\mathbf{R}_{\mathrm{inelastic}}$ contain the implementation of the multifluid algorithm through the $b_{iF}(\phi)$ function. $b_{iF}(\phi) = 1$ if the plasma potential at the location in the computational domain where the equation is evaluated falls within the bracket defined for *iF* (with $b_{iF}(\phi) = 0$ otherwise). If this is the case, the population *iC, iF* increases its density thanks to electron-impact ionization of neutrals, $\dot{n}_{iz,0\to iC,iF}$. CEX reactions undergone by ions of any population with the same charge *iC* also result in an increase (given by the sum of the CEX rates $\dot{n}_{\mathrm{CEX},iC,jF}$) in the density of the population *iC, iF* when $b_{iF}(\phi) = 1$. Each population *iC, iF* also losses ions through CEX [which are recovered if $b_{iF}(\phi) = 1$] and through electron-impact ionization to charge states higher than *iC* and gains ions through the latter mechanism from charge states lower than *iC* ($\dot{n}_{iz,jC\to iC,iF}$ terms). The change in fluid momentum due to these reactions is consistently reflected in the inelastic drag term $\mathbf{R}_{\mathrm{inelastic},iC,iF}$, where $\mathbf{u}_n$ is the velocity of neutrals. Ionization rates are computed using the expression

$$\dot{n}_{iz,jC\to iC,iF} = n_e n_{jC,iF}\bar{c}_e\sigma_{jC,iC} \tag{6}$$

where n_e is the electron density, $\bar{c}_e$ is the mean thermal velocity of electrons, and $\sigma_{jC,iC}$ is the effective cross section of collisions, computed using the data from [20]–[22]. CEX rates follow:

$$\dot{n}_{\mathrm{CEX},iC,iF} = n_n n_{iC,iF} u_{iC,iF,n}\sigma_{\mathrm{CEX},iC,iF} \tag{7}$$

with n_n the neutral density, $u_{iC,iF,n}$ the relative drift velocity between neutrals and ions of species *iC, iF*, and $\sigma_{\mathrm{CEX},iC,iF}$ the effective cross section [23]. These expressions are discretized employing an Eulerian finite-volume cell-centered algorithm with implicit time stepping over the whole computational domain [24]. This last feature enables substantial savings in computational cost as time steps can be increased beyond the limits imposed by numerical Courant conditions. The momentum equation assumes that the Hall parameter for ions is very small, and therefore the magnetic field term in Lorentz's force can be neglected. Hall2De also offers the possibility of replacing one or more low-energy fluids with a PIC algorithm, in which particles are generated using the DSMC. The same bracket criterion for ion production is applied to PIC species. Due to typical Debye lengths being approximately an order of magnitude lower than the distance from the origin [5], [6], [10], quasi-neutrality is assumed, which allows for computing the plasma density directly once the density of all the ion species is known

$$n_e = \sum_{iF=1,nF}\sum_{iC=1,nC} iC\, n_{iC,iF}. \tag{8}$$

Note that this assumption may fail in the proximity of spacecraft surfaces due to the presence of a sheath.

Electron temperature and plasma potential are required to fully determine the properties of the plasma. In Hall2De, an energy equation is solved in order to determine temperature

$$\begin{aligned}\frac{3}{2}q_e n_e\frac{\partial T_e}{\partial t} = {} & \mathbf{E}\cdot\mathbf{j}_e + \nabla\cdot\left(\frac{5}{2}T_e\mathbf{j}_e + Q_e\right) \\ & - \frac{3}{2}T_e\nabla\cdot\mathbf{j}_e - \sum_s\Phi_s + Q_e^T\end{aligned} \tag{9}$$

where T_e is the electron temperature expressed in electronvolts, q_e is the absolute value of the electron charge in coulombs, $\mathbf{j}_e$ is the electron current density, Q_e is the heat flux by particle diffusion, and Φ_s and Q_e^T account for ionization and volumetric heat losses, respectively. Note that the electron current density is not known unless Ohm's law is employed

$$\mathbf{E} = \eta\mathbf{j}_e + \eta\Omega_e\mathbf{j}_e\times\boldsymbol{\beta} - \frac{\nabla p_e}{q_e n_e} + \eta_{ei}\bar{\mathbf{j}}_i \tag{10}$$

with $\boldsymbol{\beta}$ an unitary vector in the direction of the magnetic field, Ω_e the Hall parameter for electrons, η the resistivity, p_e the electron pressure, $\bar{\mathbf{j}}_i$ the averaged ion current density, and η_{ei} the effective ion resistivity. Please refer to [4] for a detailed description of the derivation of this equation. The closure of this system of equations is provided by the current conservation equation

$$\nabla \cdot \left(\mathbf{j}_e + \sum_{iF=1,nF} \sum_{iC=1,nC} \mathbf{j}_{iC,iF} \right) = 0 \tag{11}$$

which allows us to determine the plasma potential when employed with (10).

Motion of neutral atoms can be considered free molecular flow as the typical mean free path is in the order of hundreds of meters for neutral densities in the order of 10^{18} particles/m^3 and temperatures of approximately 700 K (thruster wall temperature). Therefore, collisions between atoms are extremely scarce and it can be considered that particles follow straight paths from the surfaces from which they emanate (i.e., anode inflow and channel walls) toward the outflow boundaries of the computational domain. In a way similar to that used in radiation problems, view factors of each of the boundary surfaces with respect to others are computed. The neutrals proceeding from each type of boundary (i.e., anode, channel walls, thruster faces, etc.) are treated as different species and straight-line paths computed. The total neutral density and velocity are reconstructed when the contributions of the multiple species are added [25]. The effect of electron-impact ionization of atoms is considered in the neutral solver with neutral density being reduced by the ionization rate.

1) Far-Plume Simplifications: Ion motion in the far-plume model is modeled making use of the isothermal hydrodynamic equations (2)–(5) with some simplifications. Due to their low relevance in the far plume, all the elastic collisions are neglected. Only those terms related to changes in density and momentum due to ionization or CEX are retained. In order to reduce the number of equations to be solved, only two fluids are considered. The high-energy fluid corresponds to the extension to the far plume of the high-energy fluid in Hall2De (i.e., $iF = 1$, the main beam). Due to the low value of the plasma potential in the far plume, new ions cannot be generated for this fluid, but ion density losses occur through CEX collisions with neutrals. Low-energy fluid ions are generated in the far plume through ionization and CEX. This second fluid uses as inflow boundary conditions the combined density and momentum fluxes corresponding to the remainder of fluids in Hall2De (i.e., $iF = 2, \ldots, nF$, where nF is the total number of fluids used in the Hall2De simulation) and the PIC ions.

The motion of charged particles in the far plume is subject to the presence of an electric field. Assuming that electron and ion currents are very small and comparable due to the first being used to neutralize the second, Ohm's law can be simplified to

$$\mathbf{E} \equiv -\nabla\phi = -\frac{\nabla p_e}{q_e n_e}. \tag{12}$$

Further simplification can be achieved when the electron temperature is considered constant (an assumption also employed when imposing the boundary conditions at the maximum radial and axial positions of the Hall2De computational domain and verified by experimental evidence [16]). This results in the classical Boltzmann's relation (i.e., barometric law)

$$\phi - \phi_0 = T_e \log\left(\frac{n_e}{n_{e0}}\right). \tag{13}$$

The use of barometric law for the plasma potential can cause very large negative values of the plasma potential as the density decreases with distance from the thruster exit. This is translated to ions being accelerated by electric fields over longer distances, resulting in unphysical kinetic energy values. A reasonably accurate fix for this problem is the modified barometric law proposed in [14]. Assuming a Maxwellian distribution, only electrons with energy beyond a certain limit value of the plasma potential can carry current. Then, in a cylindrical geometry around an isotropic source of electron current, we obtain

$$j_e = q_e n_e \sqrt{\frac{q_e T_e}{2\pi m_e}} \left[1 - \frac{\phi - \phi_\infty}{T_e}\right] \exp\left(-\frac{\phi - \phi_\infty}{T_e}\right) \tag{14}$$

with j_e the absolute value of electron current in the radial direction and ϕ_∞ the limit plasma potential. All the parameters of the right-hand side term are evaluated at the source point. The inflow boundary of the plume model may be assimilated to a point source, and the ion current at the boundary can be used to compute the electron current since we impose as an outflow boundary condition of Hall2De

$$\mathbf{j}_e = -\sum_{iF=1,nF} \sum_{iC=1,nC} \mathbf{j}_{iC,iF}. \tag{15}$$

Then, adding the contribution of all the edges in the inflow boundary of the plume model, we are able to obtain an expression that can be solved for the plasma potential at infinity by means of a Newton–Raphson solver

$$\begin{aligned} \left| \sum_{b,\text{in}} \mathbf{j}_e \cdot \mathbf{n}_b A_b \right| &= \left| \sum_{b,\text{in}} \sum_{iF=1,nF} \sum_{iC=1,nC} \mathbf{j}_{iC,iF} \cdot \mathbf{n}_b A_b \right| \\ &= \sum_{b,\text{in}} q_e n_{e,b} \sqrt{\frac{q_e T_{e,b}}{2\pi m_e}} \left[1 - \frac{\phi_b - \phi_\infty}{T_{e,b}}\right] \\ &\quad \times \exp\left(-\frac{\phi_b - \phi_\infty}{T_{e,b}}\right) A_b \end{aligned} \tag{16}$$

where A_b is the boundary edge area, $\mathbf{n}_b$ is the normal to the edge, and suffix b for plasma variables denotes evaluation at boundary edges. The corrected barometric law reads

$$\phi - \phi_\infty = T_e \log\left(\frac{n_e}{n_{e\infty}} + 1\right) \tag{17}$$

where $n_{e\infty}$ has been chosen in a way such that the density n_e corresponds to the plasma density found on the edge $b_{\max}$

at which the plasma potential had the largest value (i.e., $\phi_{b\max} = \max_b \phi_b$). Consequently

$$\eta_{e\infty} = \frac{\eta_{e,b_{\max}}}{\exp\left(\frac{\phi_{b_{\max}} - \phi_\infty}{T_e}\right) - 1}. \tag{18}$$

Note that T_e is the constant electron temperature value, measured in electronvolts, in the far-plume domain. Test simulations with the aim of comparing the results obtained with barometric law and the modified formulation in (17) were conducted and revealed that barometric law produces a higher divergence angle of the beam as ions are drawn to regions of very low potential.

Finally, the neutral gas motion is solved in the same manner as in Hall2De. In order to do this, the momentum flux of neutrals is required at the boundary between Hall2De and the plume model.

C. Boundary Conditions

Three distinct boundaries are specified in the computational domain (see Fig. 2). Conditions at the centerline are such that mass and momentum fluxes cannot traverse the boundary. Outflow conditions assume that conditions at the boundary do not change with respect to the state encountered in the closest cell to the boundary (i.e., zero-gradient boundary conditions). Inflow boundary conditions need to be interpolated from Hall2De simulations. In order to solve the mass and momentum equations from each ion species (i.e., high- and low-energy fluids, each with three charge states), the following fluxes need to be specified at each edge of the inflow boundary:

$$F^n_{b,iC,iF} = n^b_{iC,iF}\mathbf{u}^b_{iC,iF} \cdot \mathbf{n}_b \tag{19}$$

$$F^{n\mathbf{u}}_{b,iC,iF} = n^b_{iC,iF}\mathbf{u}^b_{iC,iF}\left(\mathbf{u}^b_{iC,iF} \cdot \mathbf{n}_b\right) + kT_i n^b_{iC,iF} \tag{20}$$

as they are used in the computation of the discrete divergence operator on the left-hand side of (2) and (4). Thus, the number density and momentum are required at each edge of the inflow boundary. The high-energy fluid conditions ($iF = 1$) can be directly read from its Hall2De counterpart. In contrast, the low-energy fluid density and momentum are found when all of the low-energy species present in Hall2De are added

$$\begin{aligned} n_{iC,1} &= n_{iC,iF(\text{Hall2De})=1}, \quad n\mathbf{u}_{iC,1} = n\mathbf{u}_{iC,iF(\text{Hall2De})=1} \\ n_{iC,2} &= \sum_{iF(\text{Hall2De})=2,nF} n_{iC,iF} + n_{\text{PIC}} \\ n\mathbf{u}_{iC,2} &= \sum_{iF(\text{Hall2De})=2,nF} n\mathbf{u}_{iC,iF} + n\mathbf{u}_{\text{PIC}}. \end{aligned} \tag{21}$$

the value of the plasma potential at the boundary edges is required to solve for the potential at infinity using (16). Electron temperature at the boundary is assumed constant and equal to that used everywhere else in the far plume. Finally, the neutral algorithm makes use of the neutral mass flux (i.e., the momentum in the direction normal to the boundary). These variables are made readily available at the edges of the Hall2De computational domain. However, these edges will not correspond in general with the inflow boundary edges of the plume model. To provide for a smooth transition between different boundary discretizations, the edge-centered quantities in Hall2De are first interpolated to the boundary vertices of the Hall2De grid. The vertex-centered data are provided to the plume model, which for each edge in the plume model boundary, will locate the surrounding Hall2De vertices and perform linear interpolation of the variables.

D. Initial Conditions

The initial conditions in the far-plume computational domain are not extremely important as we are seeking a steady-state solution of the system of equations to which any initial condition will converge in some amount of time. For simplicity, it is assumed that the ion velocity field is initially zero and that the ion density follows a $1/(r^2 + z^2)$ decay from the density value at the inflow boundary as distance from the thruster increases along a ray. Before proceeding with time stepping for the ion motion equations, the neutral gas equations are independently evolved to the steady state. The reason for this being that as neutrals equilibrate in a longer time than ions, the computational time required for evolving the neutral solution independently of the ion motion is much less than the cost of solving the ion algorithm and neutral algorithms together.

III. Results and Discussion

We make use of Hall2De simulations of the H6 Hall thruster (Fig. 3) for obtaining the required inflow boundary conditions required in the plume model. This thruster was developed in a joint effort of the University of Michigan, the Air Force Research Laboratory, and the JPL. The H6 [26], [27] is a 6-kW class with a centerline-mounted cathode thruster designed for nominal operation at 300 V, a discharge current of 20 A, and a 20-mg/s flow rate. Under these conditions, 400 mN of thrust are achieved with a specific impulse of approximately 1950 s and total efficiency of 68.5%. Far-plume maps based on these nominal conditions are reported below. The H6 thruster was selected due to the large amount of experimental measurements in the near plume (and even in the acceleration channel) available. The experimental measurements are relatively well matched in the Hall2De simulations, as can be observed in Fig. 4, where we show a comparison with the electron temperature along the channel centerline and with the plasma potential slightly downstream of the channel exit. Unfortunately, far-plume plasma measurements are not readily available in vacuum conditions and all the far-plume data to which we have access are contaminated with backpressure effects typical of earth-based vacuum facilities. Nonetheless, we would like to stress that making use of a physics-based solver for the plasma parameters in the near plume (to approximately 20 cm from the channel exit) that can replicate experimental measurements is a key advantage of our methodology over other approaches, such as EPIC, that solve a set of simplified equations right from the cannel exit. Simulations were run with a grid resolution of 40×40, which showed a good compromise between numerical accuracy (demonstrated through a series of convergence rate tests at different resolutions) and computational cost.

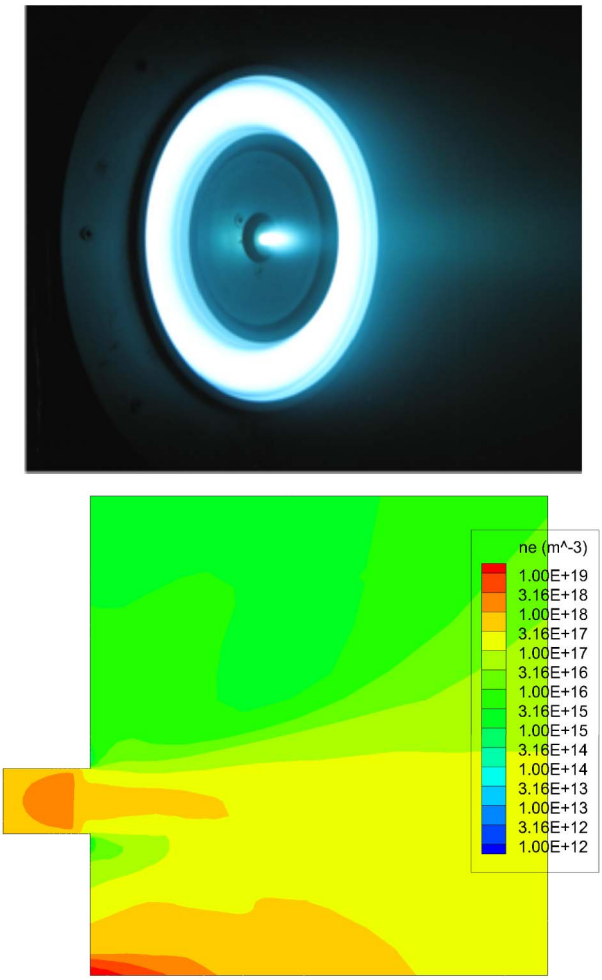

Fig. 3. H6 Hall thruster and plasma density contour from Hall2De simulation at nominal conditions.

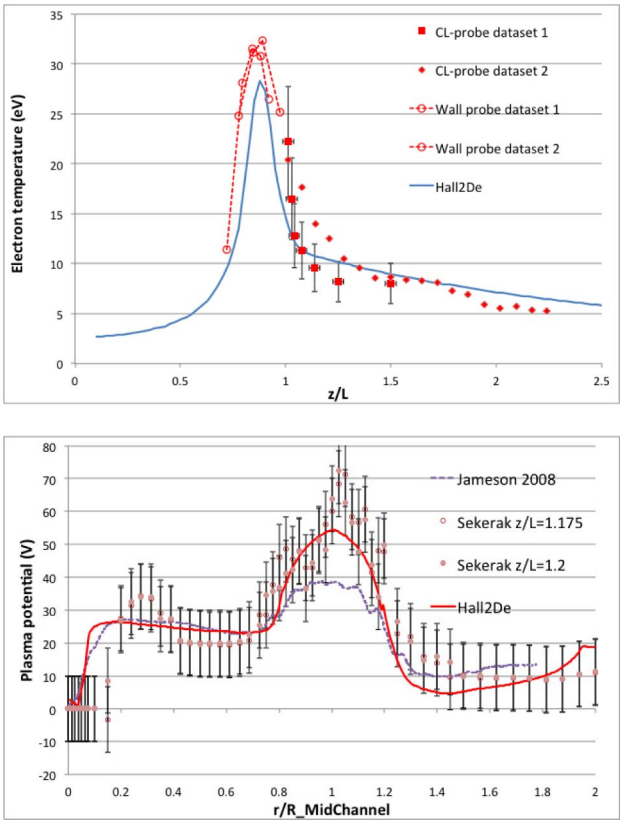

Fig. 4. Comparison of experimental measurements and Hall2De results. Top: electron temperature at the channel centerline, with L being the channel length. Bottom: plasma potential downstream of channel exit at $z/L = 1.18$.

We compare the results obtained with our plume model algorithm with those generated by the EPIC software [11], [12]. The first column of contour plots in Fig. 5 was obtained using the boundary conditions provided by a Hall2De simulation that made use of a fluid approach for high-energy beam ions and PIC for the low-energy ions. The second column of contour plots was generated using a Hall2De simulation in which two distinct fluids were used for high- and low-energy ions, respectively. The third column in Fig. 5 shows the results produced by the EPIC software. Azimuthal profiles (with 0° being the thruster centerline in the direction of the beam) of the density, ion current density, and mean energy of ions are shown in Figs. 6–8 for distances of 1 and 16 m from the thruster exit.

Concerning high-energy ions (i.e., ions that were accelerated in the thruster channel), a major difference between the solution provided by EPIC and our far-plume model is that the main beam is more divergent in the EPIC results. This is attributed to the fact that EPIC makes use of an assumed velocity profile at the channel exit derived from the experimental measurements of the SPT-140 thruster and scaled to the particular operating conditions of the thruster being tested (in this case, the H6). The SPT-140 was developed before beam-focusing techniques were investigated, and, in consequence, its beam profile is highly divergent. The different beam expansion between our simulations and EPIC are clearly observed in the second row of Figs. 5 and 6 and the first row of Fig. 7. In our simulations, the density decreases by four orders of magnitude in 40°, while the same decrement takes 55° in the EPIC results. The results in Fig. 8 reveal that the mean energy of beam ions is approximately the same in all the simulations. The two simulations generated with our code make use of the solution to the hydrodynamic (i.e., fluid) equations obtained by Hall2De as boundary conditions to propagate the solution in the plume and, in consequence, their results for high-energy ions do not differ significantly.

With respect to low-energy ions, we observe in all the simulations two separate regions of high concentration of particles. Ions at azimuthal angles from 60° to 120° are generated through ionization and CEX of beam ions a few millimeters downstream of the channel exit and accelerated in an almost radial direction by the plasma potential in the near plume. The plasma potential in the near plume is computed in the Hall2De algorithm based on the vector form of Ohm's law (10) and takes into account the presence of the magnetic field, which is not considered in EPIC. This leads to substantial differences in the near-plume plasma potential contours shown in Fig. 9, which in turn affect the far-plume results. Another effect not captured in EPIC is the

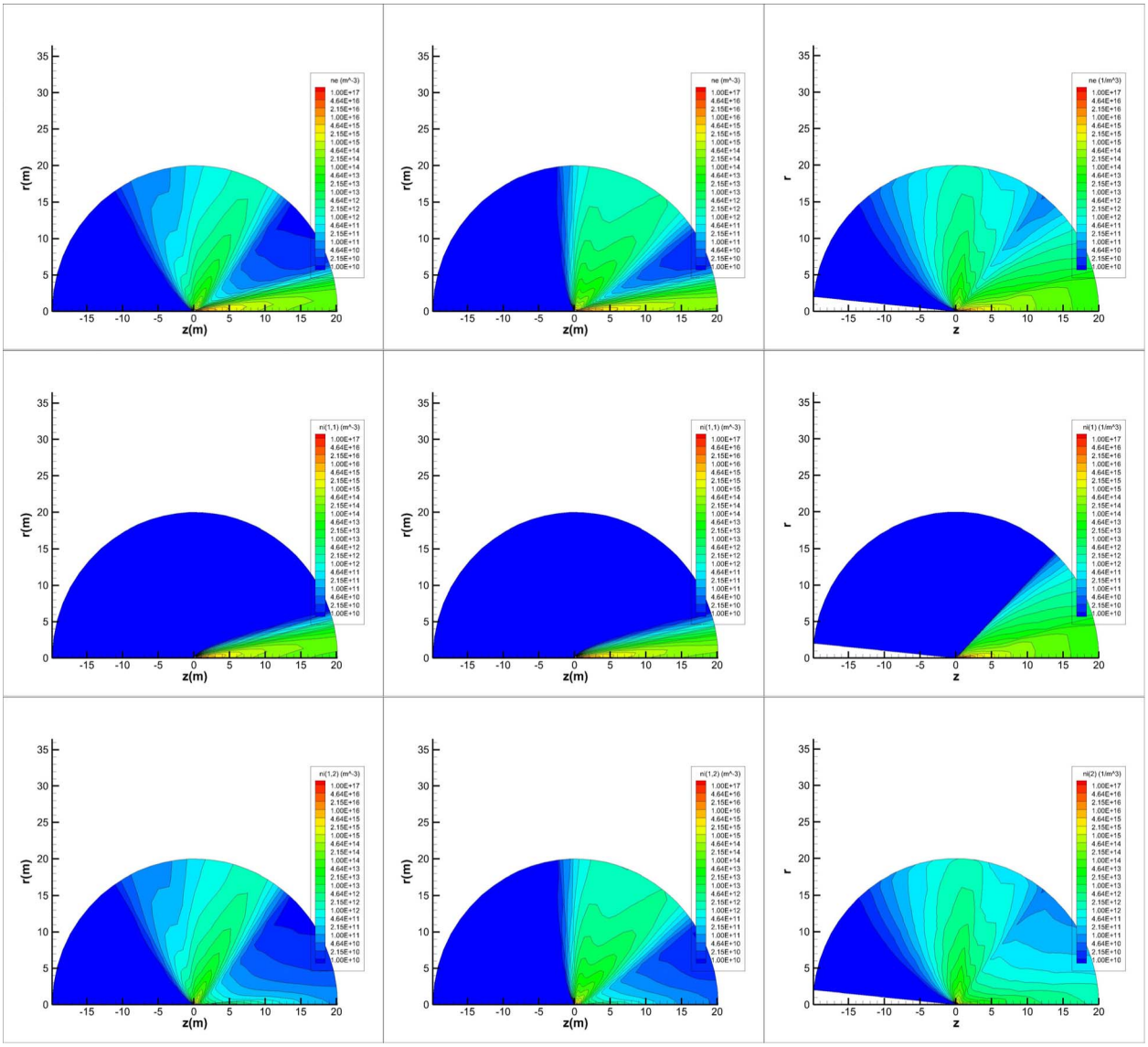

Fig. 5. Density contours for plasma density (first row), singly charged high-energy (>50 V) ions (second row), and singly charged low-energy (<50 V) ions (third row) for plasma model using 1-fluid + PIC Hall2De simulation (first column), plasma model using 2-fluid Hall2De simulation (second column), and EPIC (third column). Note that EPIC aggregates doubly and triply charged ions with singly charged ions.

contribution of ions generated in the cathode region, which can also expand radially. The second region of concentration of low-energy ions occurs around the thruster centerline (i.e., 0° of azimuth). Charged particles in this region are mostly generated through CEX reactions of beam ions far from the acceleration channel. Some cathode ions can also be accelerated in the axial direction. All the simulations present a sharp gradient in the density between the two regions described above. This phenomenon is a result of the gradient in the plasma potential at the edge of the main beam and the different generation source of ions across the gradient (ionization close to channel exit and CEX from the main beam for the first and second regions, respectively).

Even when the two regions described above are clearly identified in our simulations and in the EPIC results (third row of Fig. 5), there exist important differences in the ion densities and currents observed. In the first region (i.e., around the radial axis), the highest concentration of ion density in EPIC occurs at angles very close to 90°, while the peak density in our simulations is at angles of 50°–80° (third row of Fig. 6). This can be explained by examining the plasma potential contours in Fig. 9. In our simulations, the plasma contours have a wedge shape, which accelerates ions in a diagonal direction. In EPIC, the plasma potential decreases radially, accelerating ions in the r-direction. It is shown in Fig. 8 that low-energy ions in our simulations have an average kinetic energy of approximately 25 eV in comparison with the 10 eV of EPIC simulations. This is consistent with the plasma potential values in the near plume shown in Fig. 9. With respect to differences between our two simulations, the one that was obtained using the outflow boundary conditions of a Hall2De simulation that employed PIC for low-energy ions exhibits more density in regions at angles greater than 90°. The PIC algorithm in

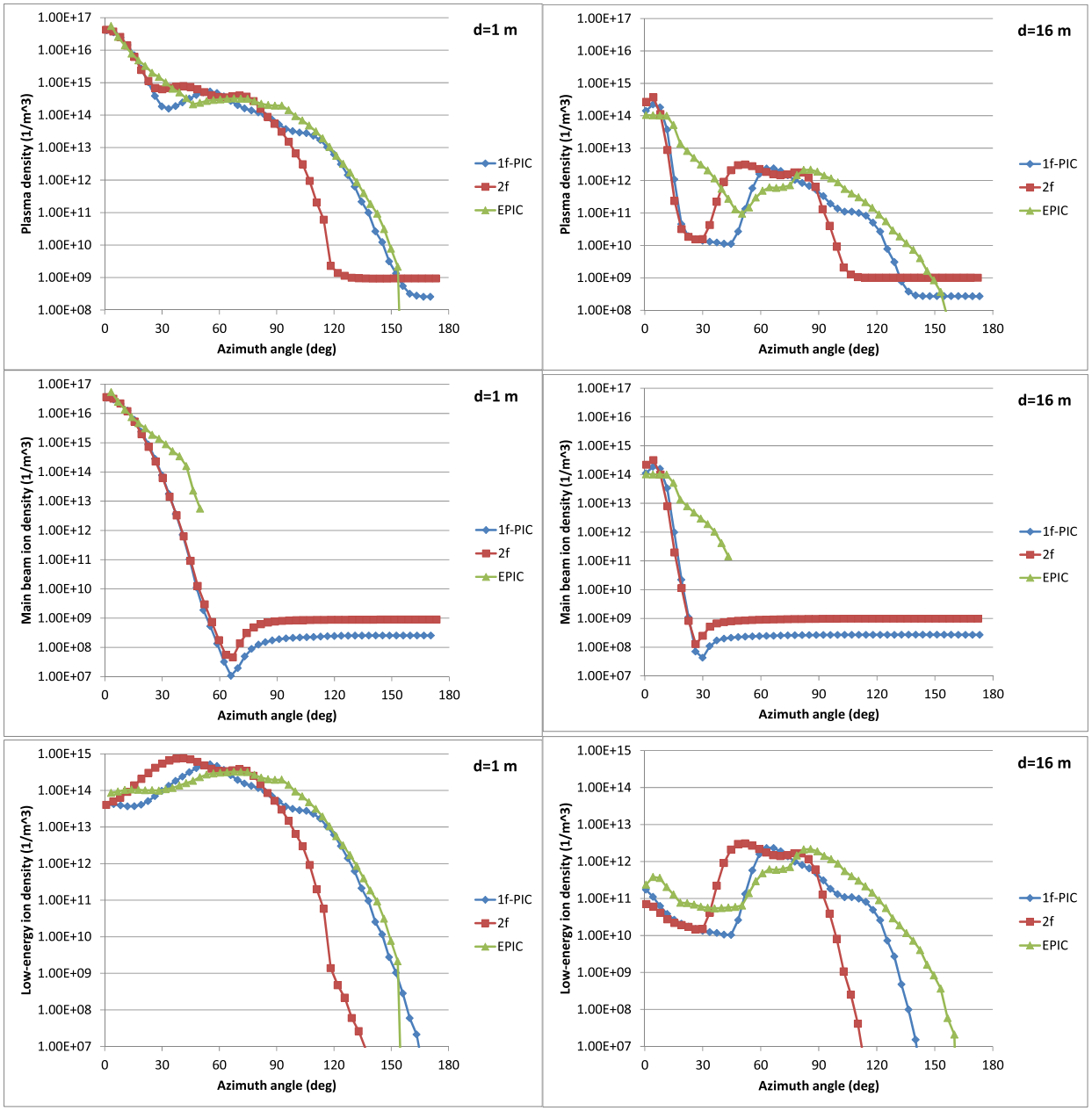

Fig. 6. Density values at distances d from origin 1 m (left column) and 16 m (right column) for plasma (first row), high-energy ions (second row), and low-energy ions (third row). Plume model results from boundary conditions obtained with Hall2De simulations of 1-fluid + PIC and 2-fluid are depicted in blue and red, respectively. EPIC results are in green.

Hall2De is able to capture some ions in the near plume that move in the direction opposite to the beam, while the averaging produced by the hydrodynamic algorithm fails to do so. The result is an outflow of ions in the 1-fluid + PIC Hall2De simulation to angles in excess of 90°.

The concentration of low-energy ions in the axial direction is larger in the EPIC results (third row of Figs. 5 and 6). The second row of Fig. 8 shows that the mean energy of these ions is in the range of 5–10 eV, which indicates that they were produced further from the channel exit that the ions found in the 90° azimuthal position. Thus, these ions are mostly produced by CEX. As shown in Fig. 1, EPIC overestimates the presence of neutral species in the plume as it neglects electron-impact ionization occurring near the channel exit. The increased neutral density enhances the occurrence of CEX reactions in the main beam.

Tables I and II show the total currents generated by ionization and CEX for our two simulations. The first important conclusion that can be extracted from these results is that the total ionization current is comparable with the CEX current in the far-plume region and inclusion of ionization effects in the equations of motion (2)–(5) is justified. Ionization and CEX in the far plume account for approximately 10% of the total current of low-energy ions with the rest being produced in

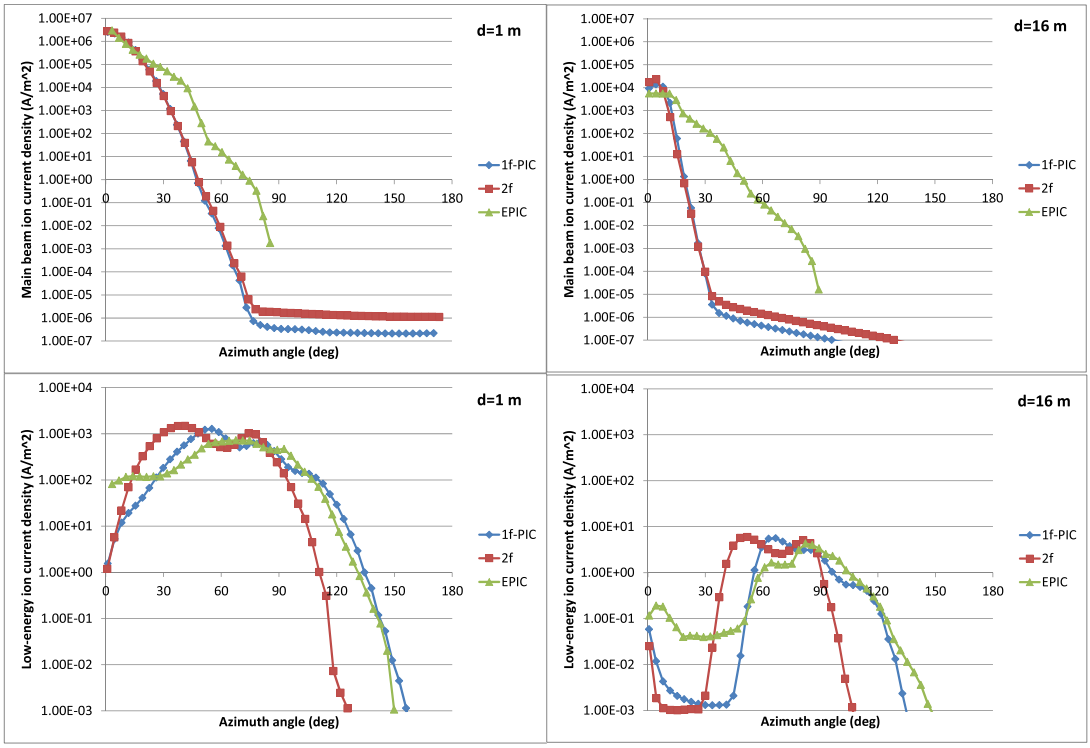

Fig. 7. Current density values at distances d from origin 1 m (left column) and 16 m (right column) for high-energy ions (first row) and low-energy ions (second row). Plume model results from boundary conditions obtained with Hall2De simulations of 1-fluid + PIC and 2-fluid are depicted in blue and red, respectively. EPIC results are in green.

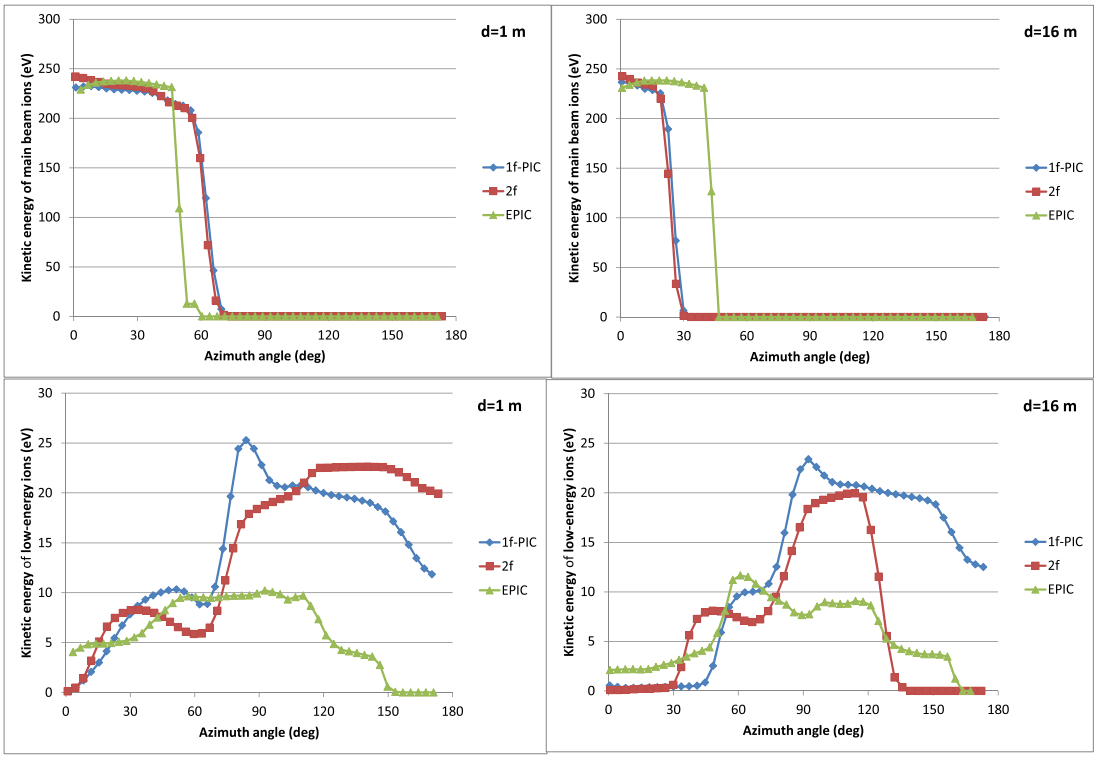

Fig. 8. Average kinetic energy of particles at distances d from origin 1 m (left column) and 16 m (right column) for high-energy ions (first row) and low-energy ions (second row). Plume model results from boundary conditions obtained with Hall2De simulations of 1-fluid + PIC and 2-fluid are depicted in blue and red, respectively. EPIC results are in green.

the near plume (Hall2De computational domain). There exist some differences in the inflow current from the Hall2De to the plume model simulation between the two cases. These can be principally attributed to the ions produced near the centered-mounted cathode, which were included with the high-energy fluid in the 1-fluid + PIC Hall2De simulation, while they

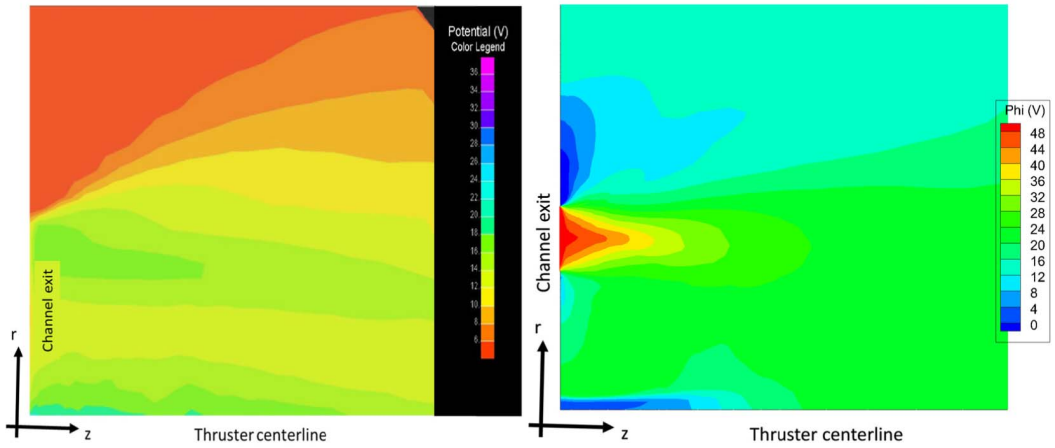

Fig. 9. Plasma potential in near plume region from EPIC (left) and Hall2De (right) simulations.

TABLE I
CURRENT FOR INFLOW BOUNDARY CONDITIONS OBTAINED WITH FLUID + PIC Hall2De SIMULATION

TOTAL CURRENT IN AMPERES A		*CHARGE*		
		+	++	+++
INFLOW	FLUID 1	14.400	2.789	0.151
	FLUID 2	0.919	$2.719 \cdot 10^{-2}$	$1.001 \cdot 10^{-3}$
IONIZATION	FLUID 1	$-1.843 \cdot 10^{-2}$	$3.652 \cdot 10^{-2}$	$5.154 \cdot 10^{-4}$
	FLUID 2	$4.087 \cdot 10^{-2}$	$2.278 \cdot 10^{-3}$	$5.974 \cdot 10^{-6}$
CEX	FLUID 1	$-6.495 \cdot 10^{-2}$	$-6.418 \cdot 10^{-3}$	$-2.328 \cdot 10^{-4}$
	FLUID 2	$6.495 \cdot 10^{-2}$	$6.418 \cdot 10^{-3}$	$2.328 \cdot 10^{-4}$

TABLE II
CURRENT FOR INFLOW BOUNDARY CONDITIONS OBTAINED WITH 2-FLUID Hall2De SIMULATION

TOTAL CURRENT IN AMPERES (A)		*CHARGE*		
		+	++	+++
INFLOW	FLUID 1	14.200	2.831	0.155
	FLUID 2	1.317	$6.975 \cdot 10^{-2}$	$1.439 \cdot 10^{-3}$
IONIZATION	FLUID 1	$-2.0142 \cdot 10^{-2}$	$3.990 \cdot 10^{-2}$	$5.800 \cdot 10^{-4}$
	FLUID 2	$3.666 \cdot 10^{-2}$	$3.847 \cdot 10^{-3}$	$1.327 \cdot 10^{-5}$
CEX	FLUID 1	$-5.537 \cdot 10^{-2}$	$-5.631 \cdot 10^{-3}$	$-2.062 \cdot 10^{-4}$
	FLUID 2	$5.537 \cdot 10^{-2}$	$5.631 \cdot 10^{-3}$	$2.062 \cdot 10^{-4}$

were included in the low-energy fluid in the 2-fluid Hall2De simulation. The reason why they were not modeled as PIC in the 1-fluid + PIC simulation is that the ion densities around the cathode are high and important collisional effects captured only by the hydrodynamic equations cannot be neglected. A more correct approach would consist of setting up a simulation with 2-fluids + PIC, where the first fluid contains beam ions, the second fluid cathode ions, and the remainder of ions in the near plume would have been modeled with PIC.

IV. CONCLUSION

We have developed a numerical algorithm for constructing the far-plume maps of HETs that works consistently with the results of numerical simulations produced by Hall2De, an algorithm that solves the equations of motion of each of the species present in the plasma by means of a full hydrodynamic approach. Major improvements with respect to previous numerical efforts include the implementation of electron–neutral ionization in the far plume, a neutral algorithm based on view factors similar to that implemented in Hall2De, and, most importantly, the determination of inflow boundary conditions for the plume model through coupling with Hall2De results in the near plume that have been validated with available experimental measurements. This approach makes possible not having to assume ion density and velocity profiles at the channel exit. Savings in computational time by making use of implicit time stepping allow us to quickly run simulations in workstation-class machines.

Comparisons with the results obtained by the plume model in EPIC revealed that a more focused beam along the thrust axis is obtained in our plume model and that the location of maximum concentration of low-energy ions moves downstream to angles of approximately 70°–80° from the centerline. These discrepancies are likely to be produced by the assumptions made by EPIC on the beam profile and the plasma potential in the near plume not being computed using the complete form of Ohm's law. We also showed some degree of uncertainty in the results depending on the method used for modeling low-energy ions in Hall2De. If a PIC algorithm is used, tracking of ions that move in the opposite direction of the beam is possible and the spatial distribution of low-energy ions moves to higher azimuthal angles from the centerline. In our opinion, using PIC in Hall2De leads to a more accurate description of the plume. Further assessment (using other thrusters and/or thrusting conditions) and validation is required to reduce the level of uncertainty of the results shown here as they indicate that the negative effect of ion sputtering on solar panels (typically collocated at 90° from the thrust axis) is reduced with respect to EPIC predictions.

ACKNOWLEDGMENT

The research described in this paper was carried out by the Jet Propulsion Laboratory, California Institute of Technology, under a contract with the National Aeronautics and Space Administration.

REFERENCES

[1] A. I. Morozov, Y. V. Esipchuk, G. N. Tilinin, A. V. Trofimov, Y. A. Sharov, and G. Y. Shchepkin, "Plasma accelerator with closed electron drift and extended acceleration zone," *Soviet Phys.-Tech. Phys.*, vol. 17, no. 1, pp. 32–37, 1972.

[2] I. G. Mikellides, G. A. Jongeward, T. Schneider, T. Peterson, T. W. Kerslake, and D. Snyder, "Solar arrays for direct-drive electric propulsion: Electron collection at high voltages," *J. Spacecraft Rockets*, vol. 43, no. 3, pp. 550–558, 2005.

[3] J. M. Fife, "Hybrid-PIC modeling and electrostatic probe survey of Hall thrusters," Ph.D. dissertation, Dept. Aeronautics Astron., Massachusetts Inst. Technol., Cambridge, MA, USA, 1999.

[4] I. G. Mikellides and I. Katz, "Numerical simulations of Hall-effect plasma accelerators on a magnetic-field-aligned mesh," *Phys. Rev. E*, vol. 86, p. 046703, Oct. 2012.

[5] D. Y. Oh and D. Hastings, "Axisymmetric PIC-DSMC simulations of SPT plumes," in *Proc. 24th Int. Electr. Propuls. Conf.*, Moscow, Russia, 1995, paper IEPC-95-160.

[6] D. Y. Oh, D. E. Hastings, C. M. Marrese, J. M. Haas, and A. D. Gallimore, "Modeling of stationary plasma thruster-100 thruster plumes and implications for satellite design," *J. Propuls. Power*, vol. 15, no. 2, pp. 345–357, 1999.

[7] C. K. Birdsall and A. B. Langdon, *Plasma Physics via Computer Simulation*. Bristol, U.K.: Adam Hilger, 1991.

[8] G. A. Bird, *Molecular Gas Dynamics*, 1st ed. Oxford, U.K.: Clarendon, 1976.

[9] A. S. Bober and N. A. Maslennikov, "SPT in Russia—New achievements," in *Proc. 24th Int. Electr. Propuls. Conf.*, Moscow, Russia, 1995, paper IEPC 95-06.

[10] I. D. Boyd and R. A. Dressler, "Far field modeling of the plasma plume of a Hall thruster," *J. Appl. Phys.*, vol. 92, no. 4, pp. 1764–1773, 2002.

[11] I. G. Mikellides, G. A. Jongeward, I. Katz, and D. H. Manzella, "Plume modeling of stationary plasma thrusters and interactions with the express—A spacecraft," *J. Spacecraft Rockets*, vol. 39, no. 6, pp. 894–903, 2002.

[12] I. G. Mikellides, R. A. Kuharski, M. J. Mandell, and B. M. Gardner, "Assessment of spacecraft systems integration using the electric propulsion interactions code (EPIC)," in *Proc. AIAA*, 2002, paper AIAA 2002-3667.

[13] J. Ashkenazy and A. Fruchtman, "Plasma plume far field analysis," in *Proc. 27th Int. Electr. Propuls. Conf.*, Pasadena, CA, USA, 2001.

[14] D. E. Parks, I. Katz, B. Buchholtz, and P. Wilbur, "Expansion and electron emission characteristics of a hollow-cathode plasma contactor," *J. Appl. Phys.*, vol. 74, no. 12, pp. 7094–7100, 1993.

[15] D. H. Manzella, "Stationary plasma thruster ion velocity distribution," in *Proc. AIAA*, 1994, paper AIAA 94-3141.

[16] S. K. Absalamov *et al.*, "Measurement of plasma parameters in the stationary plasma thruster (SPT-100) plume and its effect on spacecraft components," in *Proc. AIAA*, 1992, paper AIAA 92-3156.

[17] R. M. Myers and D. H. Manzella, "Stationary plasma thruster plume characteristics," in *Proc. 23rd Int. Electr. Propuls. Conf.*, Seattle, WA, USA, 1993, paper IEPC 1993-096.

[18] D. H. Manzella and J. M. Sankovic, "Hall thruster ion beam characterization," in *Proc. AAIA*, 1995, paper AIAA 95-2927.

[19] V. M. Gavryushin and V. Kim, "Effect of the characteristics of a magnetic field on the parameters of an ion current at the output of an accelerator with closed electron drift," *Soivet Phys.-Tech. Phys.*, vol. 26, no. 4, pp. 505–507, 1981.

[20] R. Rejoub, B. G. Lindsay, and R. F. Stebbings, "Determination of the absolute partial and total cross sections for electron-impact ionization of the rare gases," *Phys. Rev. A*, vol. 65, p. 042713, Apr. 2002.

[21] E. W. Bell, N. Djurić, and G. H. Dunn, "Electron-impact ionization of In^+ and Xe^+," *Phys. Rev. A*, vol. 48, pp. 4286–4291, Dec. 1993.

[22] A. Borovik, Jr., J. Rausch, J. Rudolph, M. Gharaibeh, S. Schippers, and A. Müller, "Electron impact ionization of xenon ions," *J. Phys., Conf. Ser.*, vol. 194, no. 6, p. 062014, 2009.

[23] J. S. Miller, S. H. Pullins, D. J. Levandier, Y.-H. Chiu, and R. A. Dressler, "Xenon charge exchange cross sections for electrostatic thruster models," *J. Appl. Phys.*, vol. 91, no. 3, pp. 984–991, 2002.

[24] A. Lopez Ortega and I. G. Mikellides, "A new cell-centered implicit numerical scheme for ions in the 2-D axisymmetric code Hall2De," in *Proc. AIAA*, 2014, paper AIAA 2014-3621.

[25] I. Katz and I. G. Mikellides, "Neutral gas free molecular flow algorithm including ionization and walls for use in plasma simulations," *J. Comput. Phys.*, vol. 230, no. 4, pp. 1454–1464, Feb. 2011.

[26] B. M. Reid, "The influence of neutral flow rate in the operation of Hall thrusters," Ph.D. dissertation, Dept. Aerosp. Eng., Univ. Michigan, Ann Arbor, MI, USA, 2009.

[27] D. L. Brown, C. W. Larson, J. M. Hass, and A. D. Gallimore, "Analytical extraction of plasma properties using a Hall thruster efficiency architecture," in *Proc. 30th Int. Electr. Propuls. Conf. (IEPC)*, Florence, Italy, 2007, paper 2007-188.

Authors' photographs and biographies not available at the time of publication.